# Development of conductive cementitious materials using recycled carbon fibres

G. Faneca[a], I. Segura[b, c*], J. M. Torrents[d], and A. Aguado[b]

[a] Escofet 1886 Ltd.

[b] Department of Construction Engineering, Universitat Politècnica de Catalunya - Barcelona Tech, C1, Barcelona 08034, Spain

[c] Smart Engineering Ltd., C/Jordi Girona 1-3, Parc UPC – K2M, Barcelona 08034, Spain

[d] Department of Electronics Engineering, Universitat Politècnica de Catalunya - Barcelona Tech, C4, Barcelona 08034, Spain

## Abstract

Conductive cementitious materials have gained immense attention in recent years owing to the possibility of achieving multifunctional materials. The usual approach has been to incorporate carbonaceous nanomaterials and/or virgin carbon fibres into cementitious matrices. This paper presents the first research devoted to the development of conductive cementitious materials using recycled carbon fibres (rCFs). Four different types of PAN-based rCFs were studied, by varying the aspect ratio and supplying characteristics, in two concrete dosages: conventional and ultra-high-performance concrete mixes. Two mixing methods—dry and wet—commonly used to fabricate fibre-reinforced concrete were considered. The results obtained in our result have shown that wet mix method achieves better

* Corresponding author: Ignacio Segura Pérez. Universitat Politecnica de Catalunya. Departament d'Enginyeria de la Construcció. Carrer Jordi Girona 1-3, Edifico C1, despacho 202. E-08034 Barcelona. SPAIN. Email: ignacio.segura@upc.edu. Tel.: +34-93-401-65-30. Fax: +34-93-405-41-35

workability of the mixes and good dispersion of the fibres. Furthermore, electrical resistivity values in the range of 3–0.6 Ω·m were obtained for rCF contents ranging from 0.2 to 0.8% in vol. The obtained results demonstrate the possibility of using rCF to develop multifunctional cementitious materials and thus enhance the possibility of using these materials from an industrial point of view. Furthermore, new possibilities are created for the recycling of carbon fibre composites to obtain high-added-value products.

**Keywords**

Conductive concrete; Recycled carbon fibre; smart cementitious materials

## 1. Introduction

Concrete is currently the most widely used construction material and is likely to remain the predominant material in the near future. It forms an integral part of global civil infrastructures, ranging from small buildings to large structures such as tunnels, long-span bridges, and offshore platforms. Moreover, most of the current infrastructure in the developed world is past its designed service-life. One in three railway bridges in Germany is more than 100 years old, as are half of London's water mains. In America, the average bridge is 42 years old and the average dam is 52 years old. The American Society of Civil Engineers rates approximately 14,000 of the country's dams as 'high hazard' and 151,238 of its bridges as 'deficient' (1). The European Innovation Partnership on Smart Cities and Communities (EIPSCC) evaluated key urban infrastructure and most cities were described as 'aged and stressed' (2).

As most of Europe's infrastructure is already built, in the near future, efforts must be made to enhance the safety, efficiency, energy consumption, structural performance, and sustainability of new and existing buildings and infrastructure. A way forward to overcome the

47 aforementioned problems could be the use of smart, multifunctional construction materials. The
48 term ‘multifunction’ was coined to highlight the ability of a material to simultaneously exhibit
49 specific desirable electronic, magnetic, optical, thermal, or other properties to satisfy previously
50 unattainable performance metrics (3). The development of smart materials and infrastructure is
51 a hot research topic and an interesting focus for public opinion. Recently, energy-harvesting
52 tiles were used during the Paris marathon of 2013 and helped to produce 4.7 kWh of energy
53 (4). Current research trends in smart cementitious materials include self-healing concrete (5,6),
54 enhanced bioreceptivity concrete (7,8), mortars with biocide characteristics (9), and
55 development of conductive cementitious materials.
56
57 The incorporation of conductive phases into cementitious matrices has been one of the most
58 popular methodologies to obtain conductive and thus multifunctional cementitious materials.
59 The early works of Chung et al. (10–13) demonstrated the possibility of developing
60 multifunctional cementitious materials by adding carbon fibres into concrete. Several studies
61 have considered this path and it is still a topic of interest. The incorporation of carbonaceous
62 materials (carbon fibres, carbon black, and carbon nanomaterials) into cement-based materials
63 has achieved a wide range of novel functionalities. Apart from self-sensing capabilities (14–
64 18), such an approach has resulted in cementitious materials with other properties, such as
65 electromagnetic shielding (19,20), self-heating (17,21–23), cathodic protection of structures
66 (24,25), and chloride removal (25,26).
67
68 Conductive cementitious materials can be obtained by incorporating different type of
69 functional materials. Han et al (27) identified up to ten different functional materials that have
70 been used up to date to develop conductive multifunctional cementitious materials, including
71 shortcut carbon fibres (CF), carbon nanotubes and nanofibers (CNT/CNF), carbon black, steel

slag, and steel fibres. The use of steel fibres presents a high potential to develop conductive cementitious materials, i.e. for de-icing applications (28), since they are actually been widely used in the civil engineering industry as sole reinforcement in structural concrete applications. However, there are some drawbacks about using steel fibres to develop multifunctional cementitious materials, since the applied current may promote the corrosion of the fibres. Thus, carbon products were used to replace steel shavings in the conductive cementitious materials mixture design (17). Among all functional materials used up-to-date, cementitious matrices with either chopped CF and CNT/CNF are the most extensively and comprehensively studied in the literature (27). More recently, other authors have also been considered the utilisation of graphene mixed with other carbonaceous materials to develop self-sensing cementitious materials (29). Along with the laboratory scale studies, there are some examples of real scale use of conductive cementitious materials in the literature. One of the first works was presented by Tuan in 2008 (28), using a mix of carbonaceous materials and steel fibres. Most of the real-scale tests were intended for de-icing applications (21,30), and for self-sensing applications (15). However, we are still far away to find multifunctional cementitious materials fully incorporated into the civil engineering industry. Recently some efforts have been made to commercialise chopped carbon fibre but the costs are significantly higher than those of other fibres used in the civil engineering industry. A possible way to achieve low-cost multifunctional cementitious materials is the use of recycled carbon fibres (rCF). Recycled carbon fibres are mainly obtained from aerospace composite scrap. Among many different methods, most of the commercially available rCF are obtained via pyrolysis. This process allow a high retention (up to 90%) of the properties exhibited by virgin carbon fibres (31,32). The use of this kind of fibres in cementitious materials has gained attention last years, as more companies have started worldwide to provide rCF in a commercial way. Most

of recycling processes yield rCF with high retention of mechanical properties (33) but with a 30 to 40 percent cost savings versus virgin carbon fibre.

The objective of this article is to evaluate the effect of different rCFs on the mechanical and electrical properties of cementitious materials. Accordingly, different types of rCFs were added with different contents (0.1 to 1.4% in volume) to conventional concrete (CC) and ultra-high-performance concrete (UHPC) dosages. The effect of the incorporation of rCF on the slump flow was evaluated. Furthermore, compressive and flexural strength measurements were obtained in concrete samples along with electrical measurements. Finally, rCF dispersion was evaluated via visual inspection.

## 2. Research significance

This study is the first research devoted to the development of conductive cementitious materials using rCF. Other researchers have studied the incorporation of rCF into polymeric matrices and evaluated their mechanical and electrical properties (34–36). Only the recent work by Nguyen et al. has evaluated the effect of these kinds of fibres on the mechanical properties of cementitious materials, but the rCFs used were reclaimed carbon fibres that were not treated to eliminate polymer residue (37,38). The main aim of this study is to provide insights into the use of rCF as a conductive phase to develop multifunctional cementitious materials. The research outcome might facilitate the development of novel multifunctional cementitious materials that can be employed in the civil engineering industry and thus modify the actual paradigm of our structures.

## 3. Materials and methods

### 3.1 Concrete mixing proportions and raw materials

Two different concrete mixing proportions were used in our study (see Table 1): a conventional concrete mix (CC) and an ultra-high-performance concrete mix (UHPC). The main difference between both mixing proportions is the granular skeleton and cement content and they were selected to evaluate the possible presence of a double percolation phenomenon. This phenomenon was firstly described by Wen et al (39) and it involves fibre and cement paste percolation, as the aggregates might determine the existence of electrical conductivity through the cement paste. They demonstrated this effect in conductive cementitious materials as the aggregates might determine the existence of electrical conductivity through the cement paste. The maximum aggregate size in the UHPC dosage is 1 mm whereas that in the CC dosage is 12 mm. The water-to-cement ratio (w/c) also differed in both mixes—0.45 in the CC mix and 0.14 in the UHPC mix.

Table 1. Concrete mixing proportions for conventional and ultra-high performance mixes

| **Component** | | **Dosage (kg/m$^3$)** | |
|---|---|---|---|
| | | **CC** | **UHPC** |
| Cement | | 400 | 800 |
| Filler | | 260 | 220 |
| Sand (0–3/0–1 mm) | | 500 | 1161 |
| Pea gravel (2–4 mm) | | 520 | -- |
| Gravel (4–12 mm) | | 400 | -- |
| Additives | Glenium B255 | 16 | -- |
| | Glenium ACE425 | -- | 30 |
| | Meyco MS685 | -- | 57 |
| Water | | 180 | 110 |

The cement selected to produce different mixtures was CEM I 53.5R. Filler was incorporated into the different dosages to achieve an optimum workability of the mixes with a low consumption of superplasticisers. The aggregates used for the CC mix were all granite and the filler was marble dust. The sand used for the UHPC mix was siliceous sand and the filler was

calcium carbonate (Betoflow). A polycarboxylate superplasticiser (Glenium B225) was used for the CC mix and the UHPC dosage used both a polycarboxylate superplasticiser (Glenium ACE425) and nanosilica suspension (Meyco MS685) to provide self-compacting characteristics to the concrete mix.

### 3.2 Recycled carbon fibres

The rCFs evaluated were PAN-based carbon fibres in all cases. The rCFs were provided by ELG Carbon Fibre Ltd. (CFRAN, C10/30, and CT12) and CAR FiberTec (CFTrim). The characteristics of all the rCFs are listed in Table 2. CFRAN and C10/30 are monofilament rCFs differing in their average length; CT12 and CFTrim are fibrillated sheets. The fibre factor, $F$, illustrates the effect of both the volume fraction and geometrical characteristics of the fibres and was first proposed by Narayanan and Darwish (40) as equation [1]:

$$F = \beta \cdot V_f \cdot L_f / d_f \quad [1]$$

where $\beta$ is the fibre shape factor (0.50 for round fibres), $V_f$ is the volume fraction of fibres, and $L_f$ and $d_f$ are the length and diameter of the fibre, respectively ($L_f$ / $d_f$: fibre aspect ratio). Both the fibre factor and mix design determine the maximum concentration of fibres in a given concrete dosage. The fibre dosage varied from 0.1% to 1.4% in volume.

Table 2. Properties of recycled carbon fibres as given by the suppliers

| **Property** | | **Value** | | |
|---|---|---|---|---|
| | **CFRAN** | **C10/30** | **CT12** | **CFTrim** |
| Diameter (μm) | 7.5 | | 7† | |
| Nominal length (mm) | 6 - 60 | 10-30 | 12 | 12 |
| Average length (mm) | 40 | 20 | 12 | 12 |
| Density (kg/m$^3$) | 1800 | | | 1760 |
| Tensile strength (MPa) | 3150 | | 4150 | 4200 |
| Young modulus (GPa) | 200 | | 252 | 240 |
| Electrical resistivity (Ω·m) | 0.103/0.34†† | | | 0.016 |

| | | | |
|---|---|---|---|
| Fibre factor (-) | $4286 \cdot V_f$ | $1428 \cdot V_f$ | $12 \cdot V_f$ |

158 † The effective diameter of the fibrillated sheets is 500 µm.
159 †† The electrical resistivity varies if the measurement is made lengthways (0.103) or across the cross-section (0.34)
160

161 **3.3 Sample fabrication**

162 Several methods, varying in complexity, are described in the literature to disperse carbon
163 fibres into cementitious matrices, although most of them are significantly different from the
164 normal practice. In this study, concrete samples were intended to be produced using a
165 fabrication procedure as close as possible to the industrial processes. Thus, the different
166 concrete mixes were fabricated at the industrial installations of the company Escofet 1886.
167 Specimens with dimensions 40x40x160 mm were fabricated from the mixes indicated in
168 Table 1 according to UNE-EN 196-1 (41). Two sets of samples were fabricated from each
169 mix—one for the mechanical measurements and the other for the electrical measurements.
170 The dispersion of carbon fibres is one of the most critical issues in the fabrication of carbon
171 fibre-reinforced cementitious materials. Many different methods are available in the literature,
172 ranging from the surface modification of the carbon fibres, the incorporation of different
173 admixtures (methylcellulose, water reducing agents, etc.), to the use of physical methods as
174 ultrasonic sonication (27,42). Our aim was to work as close as possible to the real practice and
175 the actual concrete compositions used in the precast concrete industry. In this work, rCFs
176 were added to the mix using two methods normally used by the construction industry to
177 manufacture fibre-reinforced cementitious materials: in the dry mix (D) after incorporating
178 the cement and aggregates and in the wet mix (W) after incorporating the water and additives.
179 Furthermore, reference samples were obtained with no addition of rCF. The electrodes used
180 for the electrical measurements were stainless steel set screws of length 5 cm, which were
181 dipped 3.5 cm into the concrete samples. Figure 1 shows a scheme on the electrodes
182 positioning on the specimens.
183

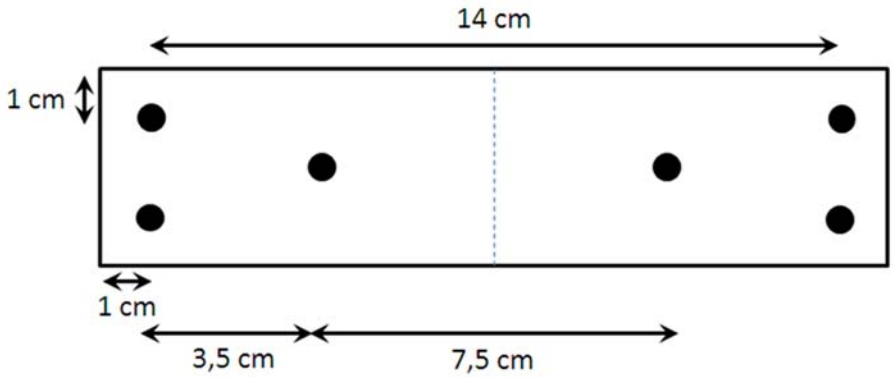


Figure 1. Location of the electrodes in the specimens

The samples were cured in a curing chamber (20° ± 2°C; 95 ± 5% relative humidity) for 28 days. The sample notation was carried out according to the following code: CC/U distinguishes between CC and UHPC (denoted as U) mixes, $C_f$ indicates the fibre content (varying from 00 for the reference sample to 14 for the sample with 1.4% fibre content), f indicates the fibre type, and M indicates the mixing method of the fibres (D or W).

$$\{CC/U\} - C_f - f - M$$

### 3.4 Characterisation methods

The slump flow was measured according to UNE-EN 1015-3 (44) prior to the elaboration of the specimens for all the mixes except CFRAN fibres. Flexural and compressive strength measurements were obtained in the concrete samples according to UNE-EN 196-1 (41); three and six replicates were made for each dosage. The electrical characterisation of the samples was performed using an Agilent HP 4192A impedance analyser and using an instrumentation amplifier as the front-end to allow 4-probe measurements (45) with an effective voltage of 1 V AC to avoid polarisation effects in the electrodes (46,47). The measurements were obtained with the frequency scanning from 10 Hz to 1 MHz, providing electrical impedance ($Z$, in Ω) and phase ($\phi$, in °). The electrical impedance is described by equation [2] and is composed of

a real part (electrical resistance, $R$) and an imaginary part (reactance, $X$). $R$ and $X$ are obtained from equations [3] and [4]:

$$Z = R + j \cdot X \quad [2]$$

$$R = Z \cdot \cos\left(\frac{\phi \cdot \pi}{180}\right) \quad [3]$$

$$X = Z \cdot \sin\left(\frac{\phi \cdot \pi}{180}\right) \quad [4]$$

Finally, the electrical resistivity ($\rho$, in $\Omega \cdot m$) is obtained using equation [5]:

$$\rho = R\frac{S}{l} \quad [5]$$

where $S$ is the effective transverse section (0.0016 $m^2$ in our study) and $l$ is the measurement length (0.07 m in our study). All the samples were allowed to reach hygrothermal equilibrium by maintaining them under laboratory conditions for 15 days after the completion of the curing period. The rCF dispersion in the cementitious matrix was evaluated by visual inspection.

## 4. Results

### 4.1 Physical and mechanical properties

The slump flow variation evaluated for different rCFs is shown in Figure 2. The slump flow was not measured in the CC-CFRAN-D samples owing to the difficulties observed during the mixing of the samples. The excess length of this rCF (which was larger than the maximum size of 60 mm provided by the supplier) and the characteristics of the concrete dosage resulted in a significant reduction in the mix workability. The data were grouped into two sets according to the mixing method. The samples with the rCF incorporated into the wet mix (W samples) exhibited slightly larger slump flow for different fibre contents. Furthermore, the rCFs provided as fibrillated sheets (CT12 and CAR) exhibited larger slump flow and thus

227 better dispersion of the fibres in the cementitious matrix than those presented as single fibres
228 (CFRAN and C10/30). For all the samples, it was observed that the slump flow was reduced
229 as the content of rCF was increased, which is consistent with the results presented in other
230 studies with virgin carbon fibres, although the mixing methods were different (16,48).
231 Considering the difficulties observed during the fabrication of the conventional concrete
232 mixes for CFRAN carbon fibres, the rest of the mixes were obtained only with the UHPC
233 mix. The fibre factor *F* of the different rCFs, as detailed in Table 2, influences the workability
234 of the mixes. There are no reported values of the fibre factor in the literature, although
235 Grunewald provided maximum values between 0.3 and 1.9 for steel-fibre-reinforced concrete
236 (49). Considering only the rCF characteristics and volume fractions, the fibre factor F varies
237 between 428 and 6000 for CFRAN, 143 and 2000 for C10/30, and 1.2 and 16.8 for CT12 and
238 CFTrim.
239

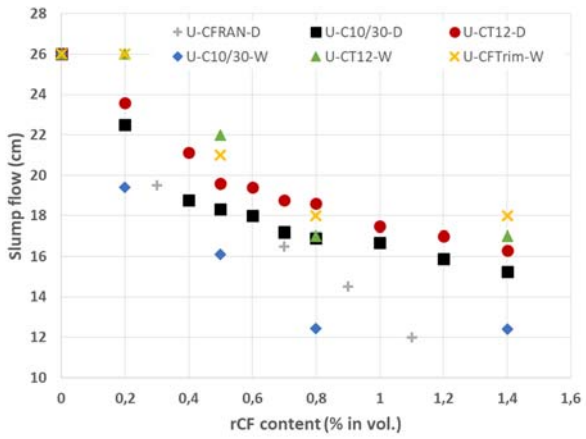


240

241 Figure 2. Variation of slump flow with the content of rCF for different mixes

242

243 The results of the compressive and flexural strength measurements (Figure 3a and b,
244 respectively) showed different behaviours of the rCF concrete samples. First, concretes made
245 with CFRAN carbon fibres exhibited a clear influence of the granular skeleton as UHPC
246 concretes exhibited larger mechanical properties than the CC concretes. As mentioned

247 previously, the incorporation of CFRAN fibres into the conventional concrete mixes resulted
248 in a large reduction in the workability. The difficulty in mixing the CC dosages influenced the
249 compactation of the samples and thus, more porosity was incorporated into the mix.
250 Therefore, these samples exhibited lower mechanical performance. Second, the mixes that
251 incorporated rCFs into the wet mix exhibited larger compressive strength than the dry mix
252 samples. This result is also consistent with the results of workability and those of previously
253 published research works (43)
254

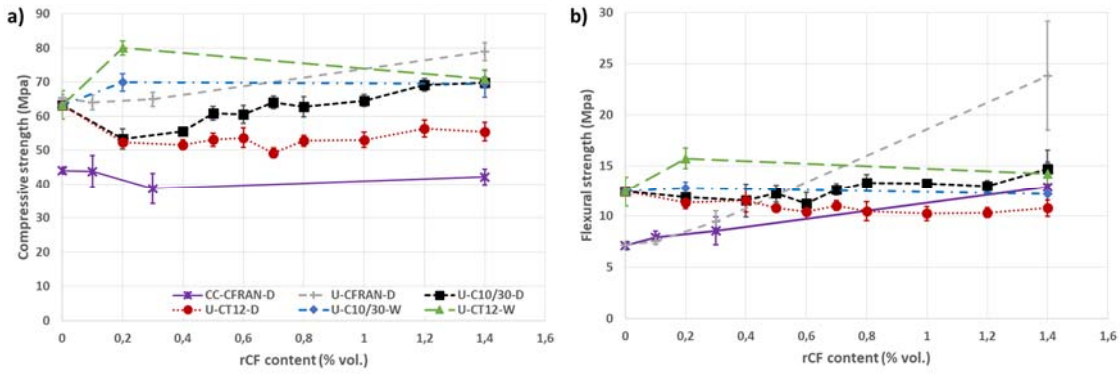


255

256 Figure 3. Variation of a) compressive and b) flexural strength with the rCF content for
257 different mixes
258

259 Finally, regarding the format of the rCF (single fibre or fibrillated sheets) and considering the
260 slump test results, larger mechanical response of CT12 samples is expected. Further, when the
261 rCFs were incorporated into the dry mix, C10/30 samples exhibited larger mechanical
262 response both in compressive and flexural strength measurements. When the rCFs were
263 incorporated into the wet mix, the trend shifted and CT12 samples exhibited larger
264 compressive and flexural strength. This result might be explained in view of the critical pull-
265 out length ($L_f^{crit}$) and number of fibres per unit volume ($N$), as recently presented by Han et al.
266 (50). In that work, critical pull-out length of carbon fibres can be got when the carbon fibres

are snapped. The authors demonstrated that, as the length of the carbon fibre decreases, $N$ increases but $L_f^{crit}$ decreases.

Figure 4 presents the variation of $N$ and $L_f^{crit}$ with the rCF content for C10/30 and CT12 fibres. More carbon fibres in the bulk matrix indicate better mechanical performance up to a certain rCF content given by the fibre factor. Once this value is reached, a further increase in the carbon fibre content might have a weakening effect owing to the presence of air voids and low dispersion of the carbon fibres. Thus, $N$ mainly influences the compressive strength. As shown in Figure 3a, C10/30 and CT12 samples exhibit almost similar compressive strength for low rCF content, because the number of fibres per unit volume is very similar (see Figure 4a). As the rCF content increases, the difference between $N$ of C10/30 and CT12 increases, and thus more defects (air voids and bundles of carbon fibres) might be present in the cementitious matrix.

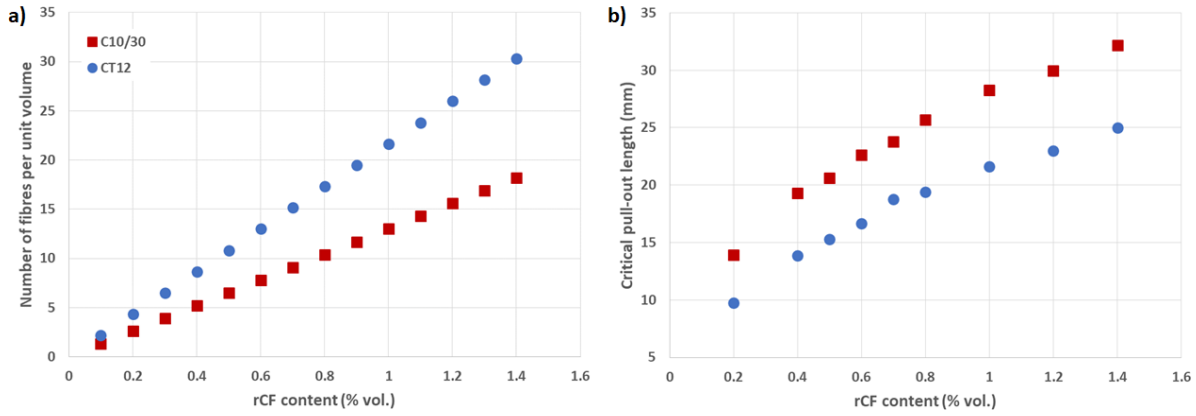


Figure 4. Variation of (a) $N$ and (b) $L_f^{crit}$ with the rCF content for C10/30 and CT12 fibres

Furthermore, the value of $L_f^{crit}$ will determine the mechanical behaviour of the carbon fibre reinforced cementitious composites. As $L_f$ increases and exceeds $L_f^{crit}$, the carbon

fibre maximum stress also increases until $L_f = L_f^{crit}$. Further increases of $L_f$ are not related to larger increases in the fibre maximum stress since the carbon fibre will be snapped from the cementitious matrix when the material is damaged. The length of both C10/30 and CT12 carbon fibres is larger than the value of $L_f^{crit}$ for almost all rCF contents (see Figure 4b). Therefore, no significant differences are expected in the flexural behaviours of the specimens as shown in Figure 3b.

## 4.2 Electrical characterisation

### 4.2.1 Effect of CFRAN fibres and influence of granular skeleton

First, the influence of the granular skeleton was verified for CFRAN fibre contents of 0.1, 0.3, and 1.4%. The Bode diagrams (impedance versus frequency) for these samples are illustrated in Figure 5. A line is drawn at 50 Hz as it is the standard frequency of electrical mains. The electrical patterns of both CC and UHPC concrete samples exhibit large differences. The plain CC specimens with no rCF addition evidence and impedance variation with frequency characteristic of an insulator material. There is almost no variation of the impedance with the increasing frequency up to 10 kHz. Once this value is reached, a large reduction on the impedance is observed. The plain UHPC concrete samples also behave as an insulator, but the variation of the impedance with frequency is different from the CC samples. Firstly, for the same frequency value, UHPC samples exhibit impedance values that are 100 to 10 times lower than the CC ones; as the frequency increases, the differences between CC and UHPC samples reduces. Secondly, the electrical pattern of the plain UHPC samples do not exhibit a drastic reduction of the impedance for frequency values above 10 kHz, but just a slight reduction in the impedance for frequencies larger than 100 kHz.

The reduction of impedance observed in the plain CC specimens are related to polarization effects. Some authors have suggested that polarization effects are not eliminated by the use of AC but are rather manifested in the form of introduction of a capacitance in parallel with the electrical resistance. As the frequency of the applied current is increased, the effect of the capacitance is reduced. The differences observed between the plain concrete samples of both CC and UHPC mixes are related to the different granular skeletons of the mixes and the percolation of the cementitious paste (47). The differences between the maximum aggregate sizes of the CC and UHPC mixes (1 mm in the UHPC mix vs. 15 mm in the CC mix) explain the different electrical patterns observed. Considering the differences observed in the electrical behaviour and the difficulties in the mixing process of the CC-CFRAN dosage, only the UHPC mix was used in the rest of this study.

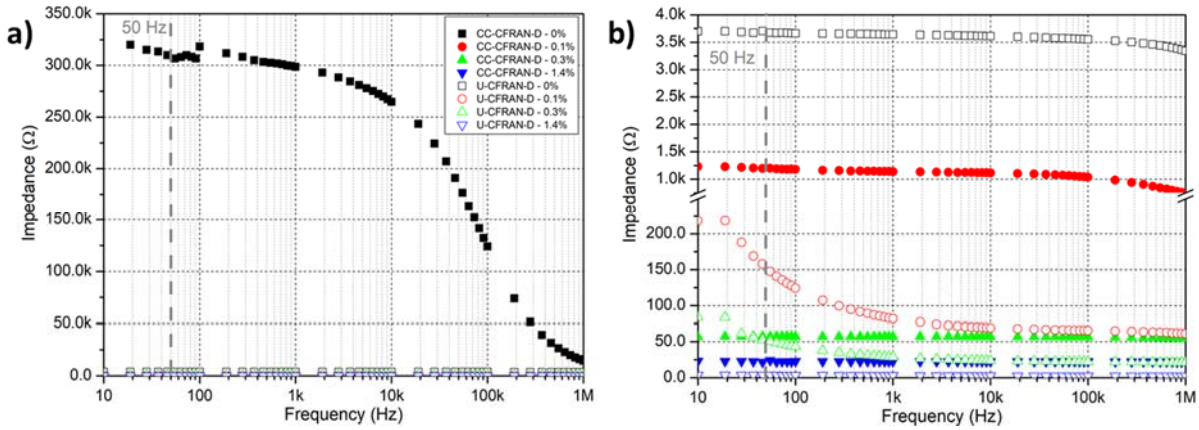


Figure 5. Bode diagrams for CC and UHPC mixes with CFRAN fibres: a) complete impedance scale, and b) 0–1300 Ω

Figure 6 shows the Bode diagrams for CFRAN fibre contents from 0 to 1.4% for the UHPC mix. The incorporation of rCF into the cementitious matrix drastically modifies the electrical behaviour of the material. The reference samples behave as an insulator with almost no variation in the impedance with the frequency. A small reduction in the impedance can be

observed only for frequencies up to 100 kHz. However, the incorporation of the rCF modifies the electrical pattern of the samples. It can be observed that the impedance is reduced as the frequency of the applied current is increased. Large reductions in the impedance values are observed as the frequency is increased up to 1–10 kHz such that the plateau appears in accordance with previous studies (51). This frequency helps overcome the effects appearing in the samples owing to the ionic conductivity of the cementitious matrix, and is referred to as the *capacitance threshold* ($C_t$).

Second, the incorporation of the CFRAN fibres drastically reduces the impedance of the samples up to the rCF content of 0.6%. Further increments in the CFRAN content do not lead to larger decreases in the electrical impedance. This electrical behaviour may demonstrate a continuous electrical path between the electrodes. The visual inspection of the fracture interfaces of the CC and UHPC concrete samples (see Figure 7) shows that CFRAN fibres tend to form bunches after mixing. The characteristics of these fibres (very high aspect ratio and supplying characteristics) did not allow good dispersion of the fibres with the standard mixing procedures used by the industry.

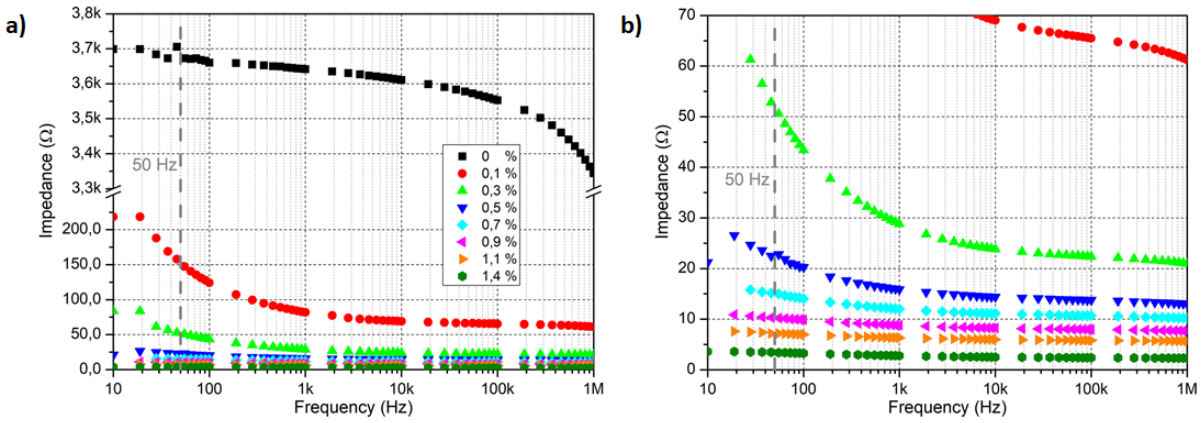


Figure 6. Bode diagrams for UHPC mixes with CFRAN fibres: a) complete impedance scale, and b) zoom-in the 0–70 Ω range of impedance

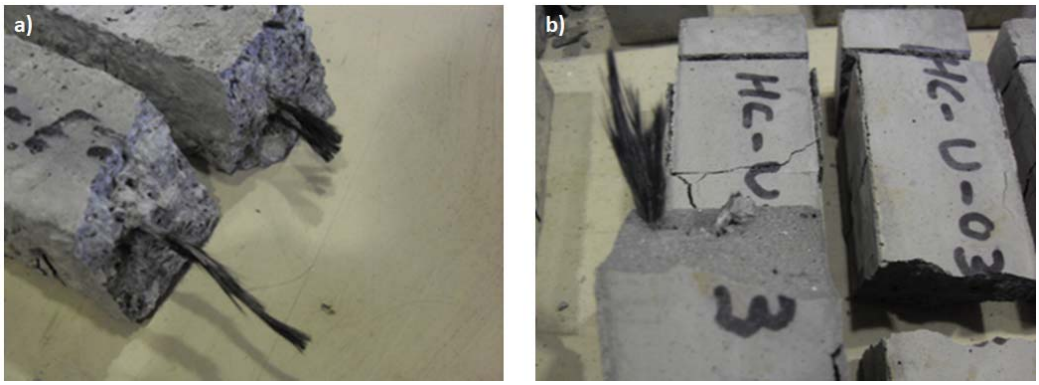


Figure 7. Presence of bunches in the CFRAN samples: a) CC mix and b) UHPC mix

### 4.2.2 Effect of C10/30 and CT12 fibres

In the case of C10/30 and CT12 fibres, the general electrical patterns obtained are similar to those observed for CFRAN fibres, as shown in Figure 8. Nevertheless, an inversion phenomenon is observed for both types of fibres. The incorporation of both types of rCFs reduces the impedance of the samples until the rCF content of 0.4–0.5% is reached. Further increases in the rCF content produce an inversion phenomenon and the impedance values increase again. In the case of C10/30 fibres (Figure 8a), the maximum impedance reduction is achieved for 0.5% content of rCF; a further increase in the rCF content results in a slight increase in the measured impedance. The CT12 fibres exhibit a more evident inversion phenomenon for rCF contents larger than 0.6% (see Figure 8b). These inversion phenomena clearly highlight the inadequate dispersion of rCF in the concrete samples.

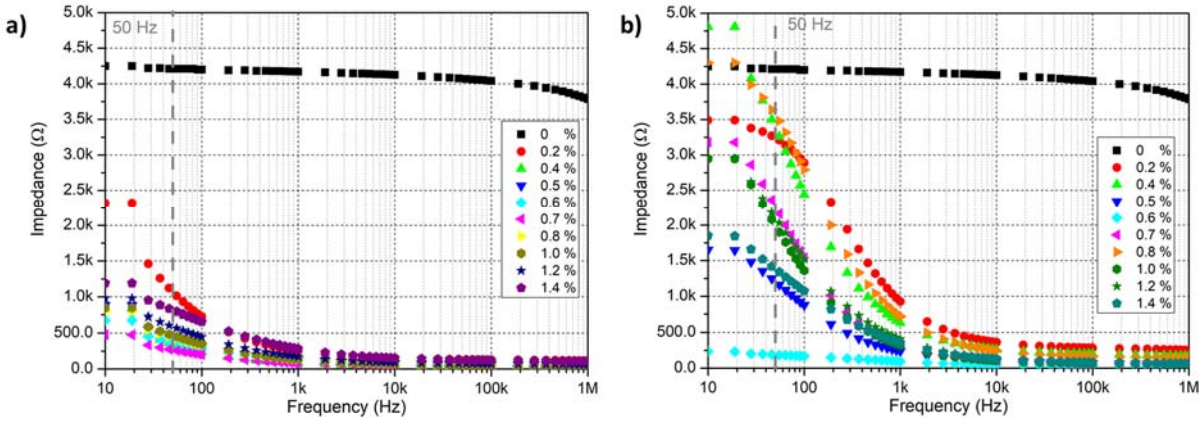


Figure 8. Bode diagrams for UHPC mixes with: a) C10/30 fibres and b) CT12 fibres

The visual inspection of the cross-section of the samples (Figure 9) also shows the presence of bunches of rCF. The distribution of rCF in the C10/30 concrete samples correlates with the impedance variation shown in Figure 8a. The number of fibres in the cross section increases up to a content of 0.6% of rCF. Bunches of rCF are observed in the cross section as the rCF content increases. The distribution of rCF in the CT12 samples presents some differences. The agglomerations of carbon fibres are observed for low contents of rCF. Nevertheless, for rCF contents larger than 0.6% no evidence of rCF can be detected in the cross section of the samples. The CT12 carbon fibres were provided as fibrillated sheets. A possible explanation for this result is the separation of the rCF sheets into individual carbon fibres or the degradation of the carbon fibres. The impedance variation for these samples (Figure 8b) may also be in accordance with a deterioration of the carbon fibres.

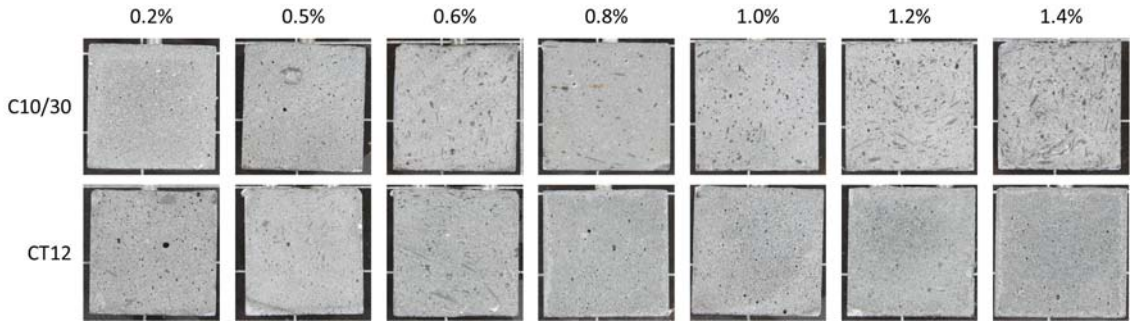


Figure 9. rCF dispersion in C10/30 and CT12 concrete samples

382

383 **4.2.3 Influence of rCF mixing method**

384 Notably, all the electrical patterns shown above correspond to rCF added to the dry mix after
385 the cement and aggregates. The effect of the mixing method on the electrical patterns is
386 illustrated in Figure 10. The incorporation of rCF into the wet mix after incorporating the
387 water and additives modifies the electrical behaviour of the samples significantly. The
388 modification affects both the impedance value and the frequency at which the impedance
389 stabilises. First, the impedance of the samples is drastically reduced when the mixing method
390 is modified. Furthermore, no inversion effect appears in the samples in the wet mix, thus
391 demonstrating good dispersion of the rCF into the cementitious matrix. The presence of
392 bunches of rCF could not be observed in the analysis of the cross-section of the concrete
393 samples (see Figure 11). Furthermore, no evidence of fibre deterioration is observed in the
394 cross section of CT12 concrete samples.

395

396 Figure 12 illustrates the variation of $Z_{CT12\text{-}D}Z_{CT12\text{-}W}$ ratio with the frequency that helps to
397 identify the effect of the mixing method on the dispersion of rCF in the cementitious matrix.
398 For rCF contents below the percolation threshold (rCF contents of 0.2 and 0.5%), the
399 influence of fibre dispersion results in a difference in impedance of the order of ten times.
400 Nevertheless, when the rCF is approximately equal to or more than the percolation threshold
401 (rCF content of 0.8%), the better fibre dispersion in the wet mix samples facilitates larger
402 differences in the electrical behaviour of the samples. Notably, once the frequency surpasses
403 the $C_t$ value, the ratio $Z_{CT12\text{-}D}Z_{CT12\text{-}W}$ stabilises at an average value of 3. Second, the
404 incorporation of the rCF into the wet mix also reduces the value of $C_t$ for different concrete
405 samples to approximately 100 kHz for the dry mix samples and 1 kHz for the wet mix
406 samples.

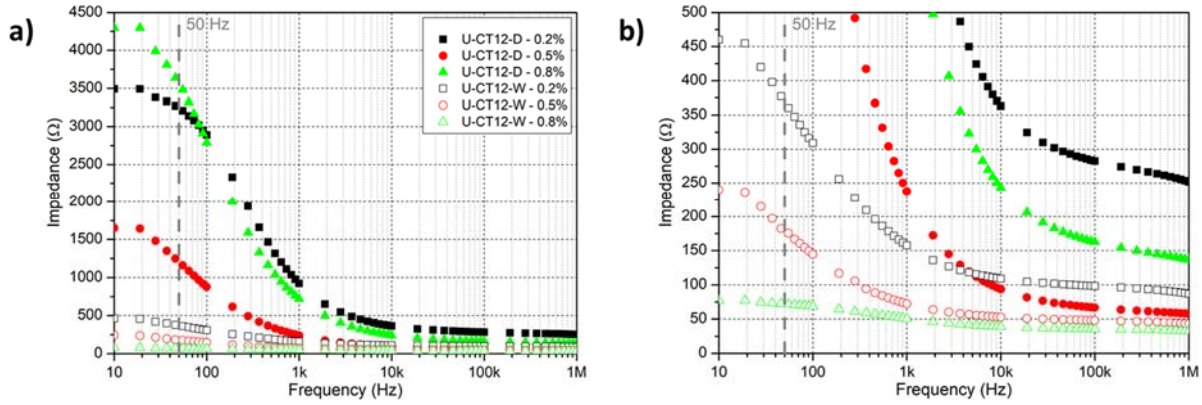


Figure 10. Effect of the mixing method on the electrical pattern of CT12 mixes: a) complete impedance scale and b) zoom-in the 0–500 Ω range of impedance

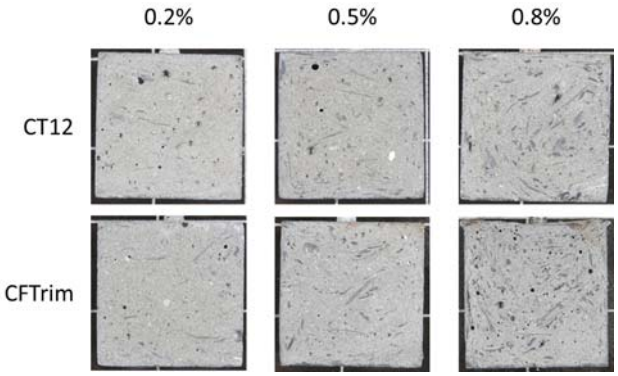


Figure 11. rCF dispersion in wet mix concrete samples

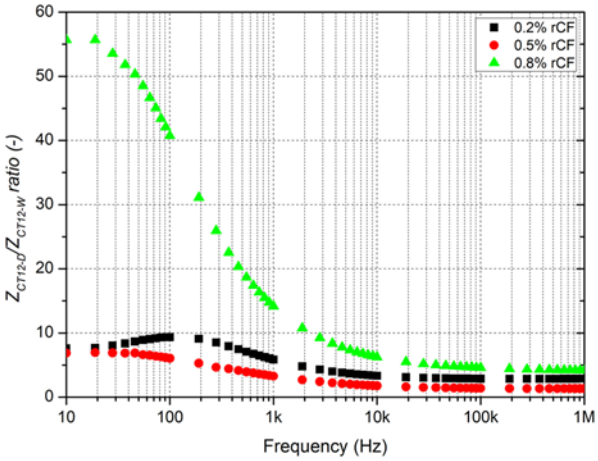


Figure 12. Variation of $Z_{CT12\text{-}D}/Z_{CT12\text{-}W}$ ratio with frequency

Furthermore, the incorporation of the rCF into the wet mix also facilitates the comparison between the electrical patterns of CT12 and CFTrim (see Figure 13). Although CT12 and CFTrim rCFs exhibit different electrical properties (see Table 2), the electrical behaviours of their equivalent concrete samples are quite similar. For rCF content of 0.8%, the percolation threshold value is reached and a continuous network of rCFs is formed in accordance with the previous studies (51). The similarities observed between the electrical patterns of CT12 and CFTrim concrete samples demonstrate that the electrical resistivity is determinate at the end by the cementitious paste that surrounds the rCF rather than by the electrical resistivity of the later.

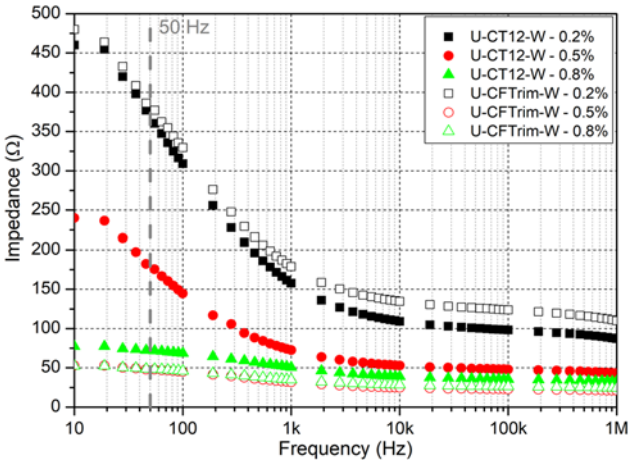


Figure 13. Comparison of the electrical behaviour of UHPC mixes with CT12 and CFTrim fibres added to the wet mix

### 4.2.4 Electrical resistivity calculation

The electrical resistivity of different concrete samples can be calculated from the measured impedance. The impedance measured, $Z$, is a complex number and thus cannot be used to determine the electrical resistivity of the samples. The electrical resistance is used instead, as described by equation [5]. As AC measurements were obtained at different frequencies, a

437 non-trivial question is to determine the frequency at which the electrical resistivity must be
438 calculated. Many authors achieved the AC characterization of carbon fibre-reinforced
439 concrete (17,50,52) but the authors only found one reference that provided the nominal
440 frequency at which the electrical resistivity was calculated. Chen et al. (51) chose 100 kHz as
441 the value of $C_t$ in their experiments. Therefore, in this work, two electrical resistivity values
442 are obtained: $\rho_{50\ Hz}$ and $\rho_{100\ kHz}$. As stated previously, $\rho_{50\ Hz}$ is of high technical importance as
443 the standard frequency for AC is 50 Hz.
444
445 The frequency selected for the electrical resistivity measurements affects the electrical
446 resistivity values as shown in Figure 14. The measurements obtained at 50 Hz clearly
447 demonstrate the influence of the fibre dispersion on the electrical resistivity of the samples
448 (see Figure 14a and b). This situation was clearly observed with U-CT12-D samples. These
449 samples exhibited inadequate dispersion of the fibres and bunches appeared after the visual
450 inspection. This was also reflected in $\rho_{50\ Hz}$ as they exhibited larger electrical resistivity
451 values. Nevertheless, the electrical resistivity of these samples measured at 100 kHz is
452 approximately 1.5 Ω·m. The lowest electrical resistivity is obtained for the wet mix rCF
453 samples (U-CT12-W and U-CFTrim-W). Furthermore, these samples are the ones less
454 affected by the chosen frequency owing to the good dispersion of fibres in the cementitious
455 matrix. The values of $\rho_{50\ Hz}$ obtained for the wet mix rCF samples are in the range of 3 to 0.6
456 Ω·m, which is consistent with the reported values for virgin carbon fibres (22,51,52).
457

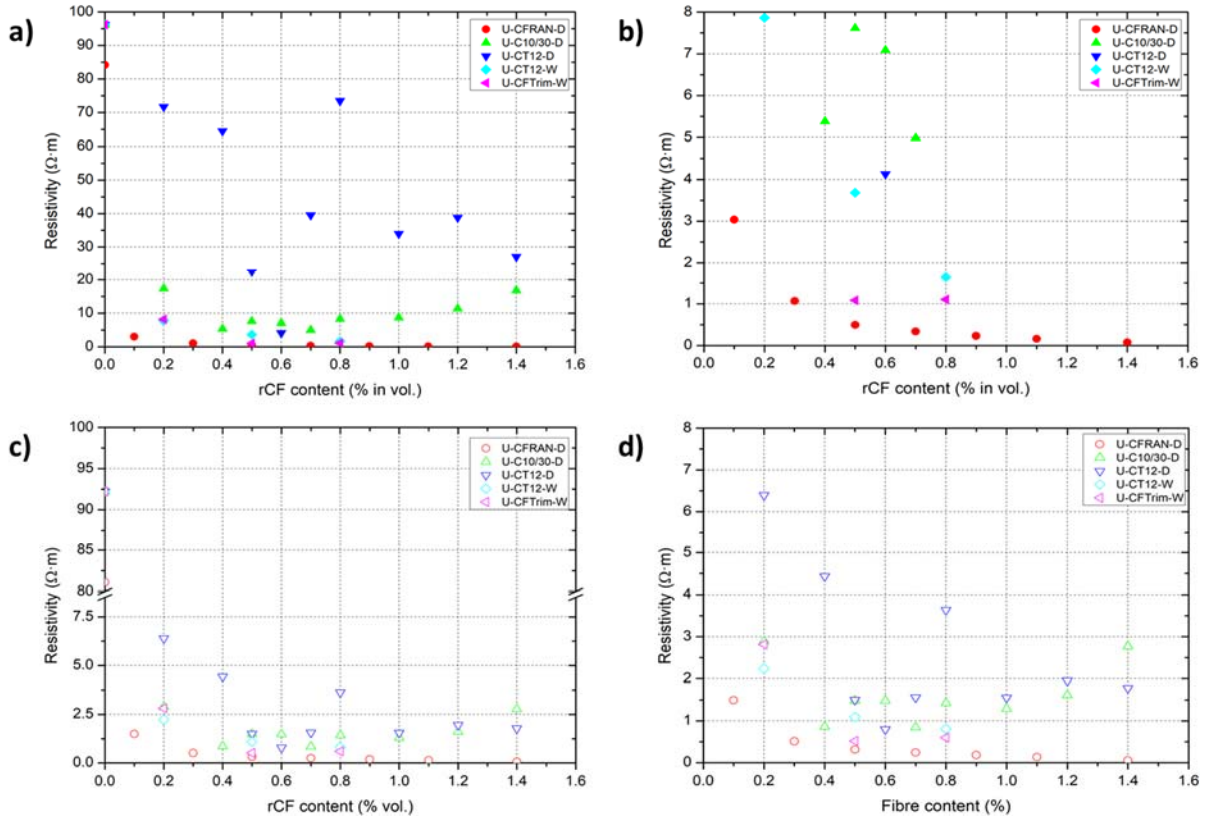


458

459 Figure 14. Electrical resistivity variation with the rCF content of different concrete samples

460 obtained at 50 Hz (a and b) and 100 kHz (c and d)

461

462 **4.2.5 Estimation of $C_t$**

463 In the different samples analysed, we have identified a 'cut-off' frequency: the *capacitance*

464 *threshold*, $C_t$. For frequency values between 10 Hz and $C_t$, there is a large variation in the

465 impedance of the samples. For frequency values above $C_t$, the impedance reaches a plateau

466 and stabilises. The values of $C_t$ vary in the range of 1 to 100 kHz depending on the type and

467 content of fibre and the mixing method. The complex impedance spectra (Nyquist diagrams)

468 of different concrete samples will be analysed to understand this question more clearly. The

469 Nyquist diagrams of cementitious materials with conductive inclusions normally exhibit three

470 individual arc/features, accounting for the electrochemical reactions and product layer

471 deposition at the electrodes and bulk-related features (53). Figure 15 illustrates the Nyquist

472 diagram for the neat UHPC concrete sample in which only two arcs can be observed. The

spur element on the right side is related to the polarisation effects at the electrode (54). The rest of the diagram is part of the arc related to the bulk response of the sample. The incorporation of the rCF modifies the diagram as shown in Figure 16. Both the reactance and electrical resistance values decrease and the feature attributed to the electrode polarization effects is not discernible, as described by previous researchers (54). Ford et al. (53) demonstrated that the Nyquist diagram of cementitious samples is affected by the inclusion of conductive phases. The emerging high-frequency arc that appears on the left side of the diagram is related to the bulk features of the sample. The other arc is characteristic of the conductive fibres (53,55).

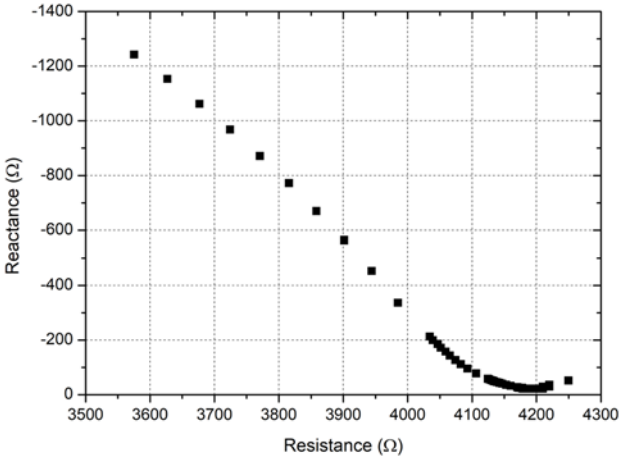


Figure 15. Nyquist diagram for the reference UHPC concrete

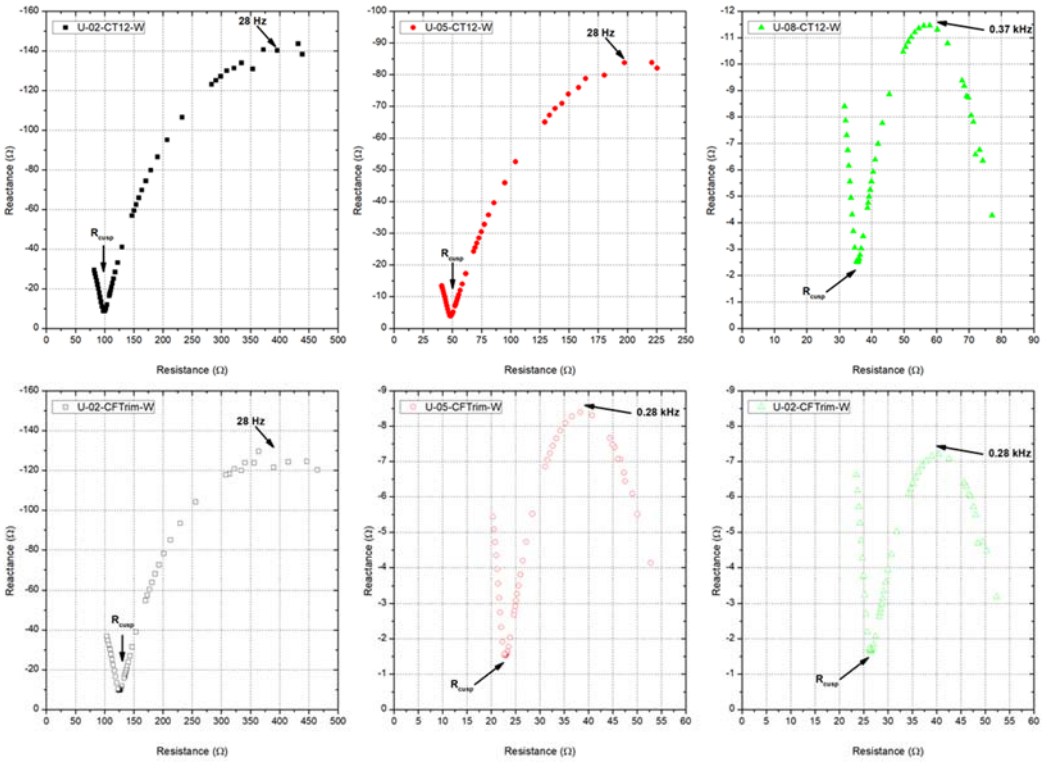


Figure 16. Nyquist diagrams for the UHPC concretes wit rCF fibres added to the wet mix

The Nyquist diagrams can also account for the rCF dispersion on the cementitious matrix as shown in Figure 17. The incorporation of CT12 fibres into the dry mix results in large increases in both the reactance and electrical resistance as compared with the wet mix samples (see Figure 16). Furthermore, the inversion phenomena caused by the build-up of the rCF is also evidenced. Two parameters can be obtained from the Nyquist diagrams: the frequency of the maximum of the arc ($f_{max}$), and the frequency and electrical resistance at the cusp-point between two arcs ($f_{cusp}$, $R_{cusp}$) as presented in Table 3 for CT12 and CFTrim concrete samples. The values of $f_{max}$ are very similar for different samples and vary between 28 Hz and 370 Hz, and are related to the rCF inclusion in the cementitious matrix. The analysis of the characteristic values of the cusp-point is also of interest. Mason et al. identified the *cusp frequency* ($f_{cusp}$) as the frequency value required to bypass the cementitious matrix that surrounds the rCF (56). There is a clear shift of the cusp electrical resistance as the rCF increases. The reduction in $R_{cusp}$ corresponds to the reduction in the outer bulk contributions

to the fibre current path. Furthermore, the values obtained for $f_{cusp}$ are very close to those indicated as the *capacitance threshold* ($C_t$). $C_t$ can be estimated from the reactance value at the cusp-point according to equation [6].

$$C_t = \frac{1}{2 \cdot \pi \cdot f_{cusp} \cdot X_{cusp}} \quad [6]$$

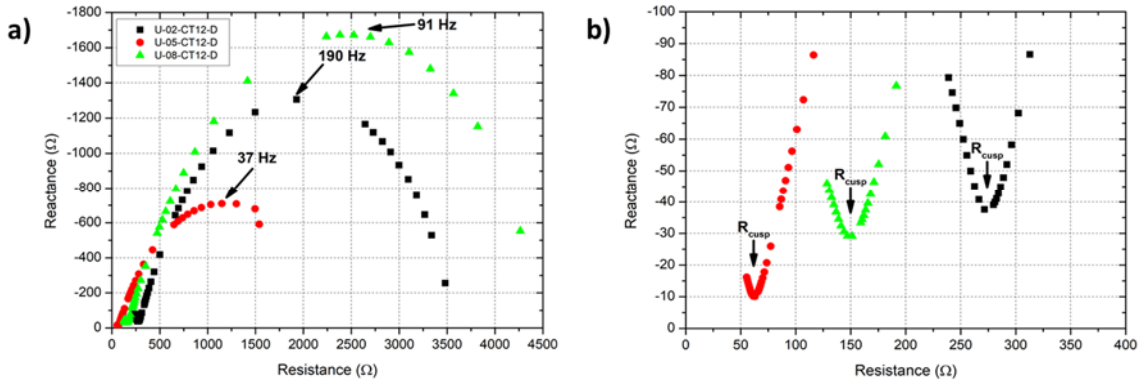


Figure 17. Nyquist diagrams for the UHPC concretes with CT12 fibres added to the dry mix

Table 3. Parameters obtained from the Nyquist diagrams of CT12 and CFTrim concrete samples

| Sample | rCF content (% in vol.) | Parameter | | | |
|---|---|---|---|---|---|
| | | $f_{max}$ (Hz) | $R_{cusp}$ (Ω) | $f_{cusp}$ (Hz) | $C_t$ (nF) |
| U-CT12-D | 0.2 | 190 | 271.6 | 190 kHz | 22.3 |
| | 0.5 | 37 | 62.9 | | 82.6 |
| | 0.8 | 91 | 151.3 | | 28.7 |
| U-CT12-W | 0.2 | 28 | 99.2 | 64 kHz | 284.7 |
| | 0.5 | 28 | 48.5 | | 637.2 |
| | 0.8 | 370 | 35.6 | 73 kHz | 868.2 |
| U-CFTrim-W | 0.2 | 37 | 125.4 | 55 kHz | 301.9 |
| | 0.5 | 280 | 22.9 | 64 kHz | 1629.3 |
| | 0.8 | 280 | 26.4 | | 1508.2 |

The values obtained for $C_t$ can be related to the '*frequency switchable model*' described by several authors (55–57). Therefore, the *capacitance threshold* can be related to the cementitious paste that coats the carbon fibres. Two adjacent carbon fibres will always be surrounded by cementitious paste. This situation can be simplified and consider the system of the carbon fibres and the cementitious paste equivalent to a parallel-plate capacitor with its capacitance $C$ defined by equation [7], where $\varepsilon$ is the permittivity, $A$ is the area of the plates, and $d$ the distance between them. If $\varepsilon$ and $A$ are assumed constant values, reductions in the distance between the plates produce an increase in the capacitance value of the system

$$C = \frac{\varepsilon \cdot A}{d} \qquad [7]$$

Consequently, as the rCF content increases and the dispersion of carbon fibres is enhanced, the distance between the fibres is reduced, as reflected by the increasing $C_t$ values shown in Table 3. Finally, the overall electrical resistance of the concrete sample is reduced.

## 5. Conclusions

This paper has demonstrated the possibility of developing conductive cementitious materials with recycled carbon fibres. This research facilitates the incorporation of multifunctional cementitious materials in the civil engineering industry, as the cost of the rCF is much lower than that of previously used carbonaceous materials. Thus, the use of multifunctional cementitious materials can be extended in actual concrete structures and not only in laboratory and small scale test applications.

Four different types of rCF were evaluated in this work. The best dispersion of the rCF was achieved for the fibrillated samples with the length of 12 mm (CT12 and CFTrim). The workability of the fresh concrete samples was significantly modified by the incorporation of the rCF, although acceptable values were obtained for the concrete samples that incorporated the rCF using the wet mix method. In terms of the mechanical performance, a reduction in both flexural and compressive strength was observed with the adding of the rCF using the dry mix method.

The electrical behaviours of different concrete samples with rCF did not differ significantly from the electrical characteristics described in the literature for concrete samples with virgin carbon fibres. The Bode diagrams of different concrete samples exhibited a common pattern. The impedance of the samples decreased as the frequency increased up to a threshold value and thereafter stabilised in a plateau. This frequency is sensitive to the fibre dispersion and is required to bypass the cementitious matrix that surrounds the rCF. The electrical resistivity values obtained for the wet mix rCF samples were between 3 and 0.6 Ω·m, which is consistent with the reported values for virgin carbon fibres.

Furthermore, we have evaluated in this work presence of a *capacitance threshold* value ($C_t$) in conductive cementitious materials.  that is related with the cementitious paste that coats the carbon fibres.

Lastly, the results presented in this article may also help boost the recycling industry of carbon fibre composites, providing new added-value applications that may be used in large structures. We are facing a world-wide problem on the recycle of obsolete aircrafts that are actually been stored in large airfields. The incorporation of rCF in multifunctional concrete

564 structures may be good contribution and will allow to enhance the sustainability of our
565 infrastructures.
566
567 Furtheremore,
568
569 **Acknowledgements**
570 The authors acknowledge the financial support provided by the Spanish Ministry of Economy
571 and Competitiveness through Project BIA2016-78742-C2-1-R, and the Torres Quevedo
572 Program (postdoctoral fellowships PTQ-14-07072 and PTQ-15-07562), as well as the support
573 from the Catalan Government through the Industrial Doctorate program DI-2015-013.
574 Furthermore, the authors wish to thank the company Escofet 1886 for their collaboration and
575 support throughout the project.
576
577 **References**
578 1. The Economist. Building works: An historic opportunity to improve infrastructure on
579 the cheap is in danger of being squandered. The Economist [Internet]. 2015; Available
580 from: https://www.economist.com/news/finance-and-economics/21662593-historic-
581 opportunity-improve-infrastructure-cheap-danger
582 2. European Innovation Partnership on Smart Cities and Communities. Strategic
583 Implementation Plan [Internet]. 2013. Available from:
584 http://ec.europa.eu/eip/smartcities/files/sip_final_en.pdf
585 3. Salonitis K, Pandremenos J, Paralikas J, Chryssolouris G. Multifunctional materials:
586 Engineering applications and processing challenges. Int J Adv Manuf Technol.
587 2010;49(5–8):803–26.
588 4. Khadilkar D. Energy-Harvesting Street Tiles Generate Power from Pavement Pounder

- Scientific American. Scientific American [Internet]. 2013 Apr [cited 2017 Aug 19]; Available from: https://www.scientificamerican.com/article/pavement-pounders-at-paris-marathon-generate-power/

5. De Muynck W, De Belie N, Verstraete W. Microbial carbonate precipitation in construction materials: A review. Ecol Eng. 2010;36(2):118–36.

6. Wiktor V, Jonkers HM. Field performance of bacteria-based repair system: Pilot study in a parking garage. Case Stud Constr Mater. 2015;2:11–7.

7. Manso S, De Muynck W, Segura I, Aguado A, Steppe K, Boon N, et al. Bioreceptivity evaluation of cementitious materials designed to stimulate biological growth. Sci Total Environ. 2014;481(1):232–41.

8. Manso S, Mestres G, Ginebra MP, De Belie N, Segura I, Aguado A. Development of a low pH cementitious material to enlarge bioreceptivity. Constr Build Mater. 2014;54:485–95.

9. Vaquero JM, Cugat V, Segura I, Calvo-Torrás MA, Aguado A. Development and experimental validation of an overlay mortar with biocide activity. Cem Concr Compos. 2016;74:109–19.

10. Chen PW, Chung DDL. Concrete as a new strain/stress sensor. Compos Part B Eng. 1996;27(1):11–23.

11. Shi ZQ, Chung DDL. Carbon fiber-reinforced concrete for traffic monitoring and weighing in motion. Cem Concr Res. 1999;29(3):435–9.

12. Chung DDL. Cement-matrix composites for smart structures. Vol. 9, Smart Materials and Structures. 2000. p. 389–401.

13. Chung DDL. Cement reinforced with short carbon fibers: A multifunctional material. Compos Part B Eng. 2000;31(6–7):511–26.

14. Chung DDL. Carbon materials for structural self-sensing, electromagnetic shielding

614 and thermal interfacing. Carbon N Y [Internet]. 2012;50(9):3342–53. Available from:
615 http://dx.doi.org/10.1016/j.carbon.2012.01.031
616 15. Liu X, Wu S. Carbon Nanotube Based Self-sensing Concrete for Pavement Structural
617 Health Monitoring. Report_University of Minesota. 2012;7(4).
618 16. Ding Y, Chen Z, Han Z, Zhang Y, Pacheco-Torgal F. Nano-carbon black and carbon
619 fiber as conductive materials for the diagnosing of the damage of concrete beam.
620 Constr Build Mater [Internet]. 2013;43:233–41. Available from:
621 http://dx.doi.org/10.1016/j.conbuildmat.2013.02.010
622 17. Gomis J, Galao O, Gomis V, Zornoza E, Garcés P. Self-heating and deicing conductive
623 cement. Experimental study and modeling. Constr Build Mater. 2015;75:442–9.
624 18. Ding Y, Huang Y, Zhang Y, Jalali S, Aguiar JB. Self-monitoring of freeze-thaw
625 damage using triphasic electric conductive concrete. Constr Build Mater.
626 2015;101:440–6.
627 19. Zornoza E, Catalá G, Jiménez F, Andión LG, Garcés P. Electromagnetic interference
628 shielding with Portland cement paste containing carbon materials and processed fly
629 ash. Mater Constr [Internet]. 2010;60(300):21–32. Available from:
630 http://materconstrucc.revistas.csic.es/index.php/materconstrucc/article/view/605/652
631 20. Micheli D, Vricella A, Pastore R, Delfini A, Bueno Morles R, Marchetti M, et al.
632 Electromagnetic properties of carbon nanotube reinforced concrete composites for
633 frequency selective shielding structures. Constr Build Mater. 2017;131:267–77.
634 21. Lai Y, Liu Y, Ma D. Automatically melting snow on airport cement concrete pavement
635 with carbon fiber grille. Cold Reg Sci Technol [Internet]. 2014;103:57–62. Available
636 from: http://www.sciencedirect.com/science/article/pii/S0165232X14000639
637 22. Galao O, Bañón L, Baeza F, Carmona J, Garcés P, Baeza JF, et al. Highly Conductive
638 Carbon Fiber Reinforced Concrete for Icing Prevention and Curing. Materials (Basel).

2016;9(4):281.

23. Wu J, Liu J, Yang F. Three-phase composite conductive concrete for pavement deicing. Constr Build Mater. 2015;75:129–35.

24. Jing X, Wu Y. Electrochemical studies on the performance of conductive overlay material in cathodic protection of reinforced concrete. Constr Build Mater [Internet]. 2011;25(5):2655–62. Available from: http://dx.doi.org/10.1016/j.conbuildmat.2010.12.015

25. Carmona J, Garcés P, Climent MA. Efficiency of a conductive cement-based anodic system for the application of cathodic protection, cathodic prevention and electrochemical chloride extraction to control corrosion in reinforced concrete structures. Corros Sci. 2015;96:102–11.

26. Cañón A, Garcés P, Climent MA, Carmona J, Zornoza E. Feasibility of electrochemical chloride extraction from structural reinforced concrete using a sprayed conductive graphite powder-cement paste as anode. Corros Sci. 2013;77:128–34.

27. Han B, Ding S, Yu X. Intrinsic self-sensing concrete and structures: A review. Meas J Int Meas Confed [Internet]. 2015;59:110–28. Available from: http://dx.doi.org/10.1016/j.measurement.2014.09.048

28. Bai YH, Chen W, Chen B, Tu R. Research on electrically conductive concrete with double-layered stainless steel fibers for pavement deicing. ACI Mater J. 2017;114(6):935–43.

29. Yoo D-Y, You I, Lee S-J. Electrical Properties of Cement-Based Composites with Carbon Nanotubes, Graphene, and Graphite Nanofibers. Sensors [Internet]. 2017;17(5):1064. Available from: http://www.mdpi.com/1424-8220/17/5/1064

30. Heymsfield E, Osweiler AB, Panneer Selvam R, Kuss M. Feasibility of Anti-Icing Airfield Pavements Using Conductive Concrete and Renewable Solar Energy. 2013.

31. Pimenta S, Pinho ST. Recycling carbon fibre reinforced polymers for structural applications: Technology review and market outlook. Waste Manag [Internet]. 2011;31(2):378–92. Available from: http://dx.doi.org/10.1016/j.wasman.2010.09.019
32. Pickering SJ. Recycling technologies for thermoset composite materials — current status. Compos Part A Appl Sci Manuf. 2006;37:1206–15.
33. Pimenta S, Pinho ST. Recycling carbon fibre reinforced polymers for structural applications: Technology review and market outlook. Waste Manag [Internet]. 2011 Feb [cited 2017 Aug 19];31(2):378–92. Available from: http://linkinghub.elsevier.com/retrieve/pii/S0956053X10004976
34. Wong KH, Pickering SJ, Rudd CD. Recycled carbon fibre reinforced polymer composite for electromagnetic interference shielding. Compos Part A Appl Sci Manuf [Internet]. 2010;41(6):693–702. Available from: http://dx.doi.org/10.1016/j.compositesa.2010.01.012
35. Turner TA, Pickering SJ, Warrior NA. Development of recycled carbon fibre moulding compounds - Preparation of waste composites. Compos Part B Eng [Internet]. 2011;42(3):517–25. Available from: http://dx.doi.org/10.1016/j.compositesb.2010.11.010
36. Akonda MH, Lawrence CA, EL-Dessouky HM. Electrically conductive recycled carbon fibre-reinforced thermoplastic composites. J Thermoplast Compos Mater [Internet]. 2013 Nov 21;28(11):1550–63. Available from: http://dx.doi.org/10.1177/0892705713513294
37. Nguyen H, Fujii T, Okubo K, Carvellu V. Cement Mortar Reinforced with Recycled Carbon Fibre and CFRP Waste. In: 17th European Conference on Composite Materials, [Internet]. Munich: European Society for Composite Materials; 2016. Available from:

https://www.researchgate.net/publication/309733808_Cement_Mortar_Reinforced_with_Recycled_Carbon_Fibre_and_CFRP_Waste

38. Nguyen H, Carvelli V, Fujii T, Okubo K. Cement mortar reinforced with reclaimed carbon fibres, CFRP waste or prepreg carbon waste. Constr Build Mater [Internet]. 2016 Nov [cited 2017 Aug 22];126:321–31. Available from: http://linkinghub.elsevier.com/retrieve/pii/S0950061816314805

39. Wen S, Chung DDL. Model of piezoresistivity in carbon fiber cement. Cem Concr Res. 2006;36(10):1879–85.

40. Narayanan R, Darwish IYS. Use of Steel Fibers as Shear Reinforcement. Struct J [Internet]. 1987;84(3):216–27. Available from: https://www.concrete.org/publications/internationalconcreteabstractsportal.aspx?m=details&ID=2654

41. AENOR. UNE-EN 196-1:2005 Methods of testing cement. Part I: Determination of strength. 2005.

42. Gao J, Wang Z, Zhang T, Zhou L. Dispersion of carbon fibers in cement-based composites with different mixing methods. Constr Build Mater [Internet]. 2017;134:220–7. Available from: http://dx.doi.org/10.1016/j.conbuildmat.2016.12.047

43. Wang C, Li K-Z, Li H-J, Jiao G-S, Lu J, Hou D-S. Effect of carbon fiber dispersion on the mechanical properties of carbon fiber-reinforced cement-based composites. Mater Sci Eng A [Internet]. 2008 Jul 25 [cited 2017 Oct 10];487(1–2):52–7. Available from: http://www.sciencedirect.com.recursos.biblioteca.upc.edu/science/article/pii/S0921509307016978?via%3Dihub

44. AENOR. UNE-EN 1015-3:2000 Methods of test for mortar for masonry. Determination of consistence of fresh mortar (by flow table). 2000.

45. Gersing E. Measurement of electrical impedance in organs measuring equipment for

research and clinical applications. Biomed Tech. 1991;36:6–11.

46. Wen S, Chung DDL. The role of electronic and ionic conduction in the electrical conductivity of carbon fiber reinforced cement. Carbon N Y. 2006;44(11):2130–8.

47. Wen S, Chung DDL. Double percolation in the electrical conduction in carbon fiber reinforced cement-based materials. Carbon N Y. 2007;45(2):263–7.

48. Yakhlaf M, Safiuddin M, Soudki KA. Properties of freshly mixed carbon fibre reinforced self-consolidating concrete. Constr Build Mater [Internet]. 2013;46:224–31. Available from: http://dx.doi.org/10.1016/j.conbuildmat.2013.04.017

49. Grünewald S. Performance-based design of self-compacting fibre reinforced concrete [Internet]. Delft University Press; 2004 [cited 2017 Aug 21]. Available from: https://repository.tudelft.nl/islandora/object/uuid:07a817aa-cba1-4c93-bbed-40a5645cf0f1?collection=research

50. Han B, Zhang L, Zhang C, Wang Y, Yu X, Ou J. Reinforcement effect and mechanism of carbon fibers to mechanical and electrically conductive properties of cement-based materials. Constr Build Mater [Internet]. 2016 Oct 30;125:479–89. Available from: http://www.sciencedirect.com/science/article/pii/S0950061816313265

51. Chen B, Wu K, Yao W. Conductivity of carbon fiber reinforced cement-based composites. Cem Concr Compos. 2004;26(4):291–7.

52. Baeza FJ, Galao O, Zornoza E, Garc??s P. Effect of aspect ratio on strain sensing capacity of carbon fiber reinforced cement composites. Mater Des [Internet]. 2013;51:1085–94. Available from: http://dx.doi.org/10.1016/j.matdes.2013.05.010

53. Ford S., Shane J., Mason T. Assignment of features in impedance spectra of the cement-paste/steel system. Cem Concr Res. 1998;28(12):1737–51.

54. McCarter WJ, Starrs G, Chrisp TM, Banfill PFG. Complex impedance and dielectric dispersion in carbon fiber reinforced cement matrices. J Am Ceram Soc.

2009;92(7):1617–20.

55. Torrents JM, Mason TO, Garboczi EJ. Impedance spectra of fiber-reinforced cement-based composites: A modeling approach. Cem Concr Res. 2000;30(4):585–92.

56. Mason TO, Campo MA, Hixson AD, Woo LY. Impedance spectroscopy of fiber-reinforced cement composites. Cem Concr Compos. 2002;24(5):457–65.

57. Hixson AD, Woo LY, Campo MA, Mason TO. The origin of nonlinear current-voltage behavior in fiber-reinforced cement composites. Cem Concr Res. 2003;33(6):835–40.